Computational Study of the Interaction between TIBO Inhibitors and Y181 (C181), K101, and Y188 Amino Acids

Renato F. Freitas and Sérgio E. Galembeck*

Departamento de Química, FFCLRP, Universidade de São Paulo, 14040-901 Ribeirão Preto-SP, Brasil

Received: May 18, 2006; In Final Form: August 18, 2006

The non-nucleoside inhibitors of HIV-1 reverse transcriptase (NNRTIs) are an important class of drugs employed in anti-HIV chemotherapy. TIBO compounds, which belong to the NNRTIs class, are potent inhibitors of the HIV-1 reverse transcriptase enzyme (HIV-1 RT). However, mutations in the amino acids present in the active site of these inhibitors limit their clinical use. In this work, the intermolecular interactions taking place between compounds of the TIBO family and Y181 (C181), K101, and Y188 amino acids are investigated. For this purpose the coordinates of three RT crystalline structures complexed with TIBO were taken from PDB database, and were analyzed by means of the B3LYP/6-31+G(d,p) model. The natural bond orbital (NBO) and atoms in molecules (AIM) methods indicate that not only does the Y181C mutation lead to loss of favorable interactions between the TIBO side chains and tyrosine, but it also affects the interaction between the inhibitor and K101 and Y188. Results also revealed that the interaction between TIBO and K101 is stabilized by N−H···O and N−H···S hydrogen bonds. This is the first time that the presence of the latter hydrogen bond (N−H···S) is reported to play an important role in the stabilization of the interaction between TIBO and K101. In addition the NBO and natural population analyses (NPA) indicate that the 8 Cl-TIBO inhibitor presents a more effective interaction with the Y181, K101, and Y188 than that of 9 Cl-TIBO.

Introduction

Infection by the human immunodeficiency virus (HIV-1), the causative agent of the acquired immunodeficiency syndrome (AIDS), is in the rank of the most terrible diseases of our history. Since the world first became aware of AIDS in the summer of 1981, the disease has spread in successive waves to various regions worldwide.[1] According to data provided by UNAIDS, the number of people infected with the HIV virus reached its highest level in 2004, when an estimated 39.4 million people were infected. In this same year, around 3.1 million people died because of AIDS around the globe.[2]

The HIV-1 reverse transcriptase (RT) enzyme is a key target in antiviral therapy because it catalyzes an essential step in virus replication: the conversion of genomic RNA into proviral DNA before it is integrated into the host genome.[3] Not only is the RT enzyme an important target for viral replication, but it also contains multiple sites to which drugs can bind. This enzyme consists of a 66 kDa subunit (560 amino acids) and a 51 kDa subunit (440 amino acids), denominated p66 and p51, respectively. Subunit p51 has the same sequence as the 440 N-terminal amino acid residues of subunit p66, which constitute the polymerase domain. Subunit p66 also contains the RNAse H domain, which is absent in p51.[4−11]

Non-nucleoside reverse transcriptase inhibitors (NNRTIs) comprise a structurally diverse series of compounds that are highly specific for HIV-1 RT inhibition.[12−14] They bind to the hydrophobic allosteric site located 10 Å away from the polymerase active site.[15] Various studies revealed a common binding mode for NNRTIs. These inhibitors lead to the rearrangement of the three β sheets of subunit p66, which contain the aspartic acid catalytic residues 110, 185, and 186. This suggests that NNRTIs inhibit HIV-1 RT by blocking the catalytic active site in such a way that it adopts an inactive conformation similar to that of subunit p51.[8,9] When bound to RT, some NNRTIs [α-APA, TIBO 86183, 9 Cl-TIBO (TIBO 82913), and nevirapine] acquire very similar conformations, which resemble the wings of a butterfly, the so-called butterfly-like conformation.[3,16] Because the RT allosteric site to which NNRTIs bind is hydrophobic, the amino acid residues surrounding the inhibitor are mostly hydrophobic, and five residues contain aromatic side chains (F227, Y318, Y181, Y188, and W229). Electrostatic interactions are rare and they involve residues K101 and K103 of subunit p66.[3,4,12]

Although NNRTIs are an important component of anti-HIV chemotherapy, their clinical use is limited by the appearance of a mutant virus resistant to these inhibitors.[12−14,16] Most of the drug-resistant mutations take place close to the binding site and are in direct contact with the inhibitor.[16,17] K103N and Y181C were the first mutations to be detected, and they confer resistance to pyridinone, nevirapine, and TIBO 82150. In fact, K103N and Y181C mutations have been observed in all NNRTIs. Other mutations include L100I, E138K, V179D, and Y188H/L.[4,16] Various studies have pursued the development of inhibitors resistant to mutations,[13,18−21] which are known as second-generation inhibitors because of their higher resistance to K103N and Y181C mutations. Some of these new inhibitors, such as capravirine, DPC083, and etravirine (TMC125),[13] are undergoing clinical trials, not to mention efavirenz, which is already in clinical use.

Analysis of the crystalline structures of the NNRTI/RT complexes in both the presence and absence of mutations is important for a deeper understanding of the interactions between the RT amino acids and the inhibitors, as well as the changes in the conformations of these inhibitors due to punctual mutations.[3,4,11,17,22−24] This analysis led to a better understanding

* Corresponding author. E-mail: segalemb@usp.br.

10.1021/jp063058u CCC: $33.50
Published on Web 10/03/2006

of why second-generation NNRTIs, like efavirenz, are less susceptible to mutations in RT. In the presence of K103N mutation, efavirenz undergoes a change in position because of a rearrangement of the allosteric site, which results in alterations in the contacts between this inhibitor and the amino acid side chains.[22,25] This molecule is also insensitive to Y181C and V106A mutations because it interacts with Y181 and V106 only weakly and forms a hydrogen bond with A106.[26] Docking and molecular dynamics studies have shown that mutations have different effects on distinct inhibitors. For example, L100I mutation has little effect on nevirapine, but it causes a 100-fold decrease in the activity of 9 Cl-TIBO because it affects the hydrogen bond between K101 and 9 Cl-TIBO and also introduces unfavorable interactions with I100.[12] Y181C and Y188H/L mutations result in the loss of favorable interactions between the amino acid aromatic rings and the aromatic portions of the inhibitor (stacking), thus generating viruses resistant to nevirapine, α-APA, and 9 Cl-TIBO.[4,17] In the case of Y188C mutation in RT, it is considered that the flexibility of the second-generation drug HBY097 greatly contributes to this inhibitor being insensitive to this mutation. The resistance mechanism with respect to loviride and HBY097 has been attributed to the stabilization of the nonbonded form of this mutant enzyme, whose allosteric site is nonexistent, thus affecting binding of the inhibitor.[27] High flexibility and facility to adopt multiple conformations have been pointed out as being the cause of the high potency of inhibitor TMC125 and diarylpyrimidine analogues (DAPY) in the face of mutations in RT.[28,29]

Various studies have also highlighted the importance of stacking and C−H/π interactions, as well as hydrogen bonds in the stability of the protein−inhibitor complexes.[30−32] Loss of these interactions has been pointed as being one of the reasons for resistance to NNRTIs.[4,16] Although these interactions play an important role in the mechanism of action of NNRTIs, studies of these interactions on the basis of quantum mechanics, which attempt at analyzing the electron density, and studies employing techniques especially developed for analysis and interpretation of these systems are scarce. For this reason, the aim of this work is to employ the potential of the techniques of electron density analysis such as natural bond orbitals (NBO),[33] natural population analysis (NPA),[34] and atoms in molecules (AIM)[35] to gain an understanding of the stabilizing or destabilizing interactions between an NNRTI and the amino acids of the allosteric site that are in contact with the inhibitor. Despite the potential applications that should arise from a clear understanding at a molecular level of the interactions between NNRTIs and the side chains of amino acids present in the inhibitory site, there are no works in the literature analyzing the electron density obtained by methods based on solutions of the Schrödinger equation for this or any other enzyme−inhibitor systems.

In this work, the intermolecular interactions of some dimers of 8-Cl TIBO or 9-Cl TIBO with one amino acid of the allosteric site were analyzed by techniques of electron density analysis. The coordinates of the dimers was obtained from the protein structures deposited in PDB. The effect of a mutation was also considered. The main objectives were: (i) to elucidate which types of noncovalent interactions occur between the TIBO inhibitor and the amino acids in the RT active site, (ii) to find out the possible causes of activity loss due to Y181C mutation, and (iii) to try to explain the reason for the higher activity of 8 Cl-TIBO when compared with 9 Cl-TIBO.

Computational Methods

Three crystalline structures of the HIV-1 RT enzyme complexed with inhibitors of the TIBO family, deposited in the *Protein Data Bank* (PDB), were used.[36] In the first structure, the enzyme was complexed with 8-Cl TIBO (1HNV) or 8-Cl TIBO (W).[4] In the second structure, the enzyme with two punctual mutations (Y181C in subunit p66 and C280S in subunit p51) was also complexed with 8-Cl TIBO (1UWB) or 8-Cl TIBO (M).[4] In the third structure, the wild enzyme was complexed with inhibitor 9-Cl TIBO (1REV).[3]

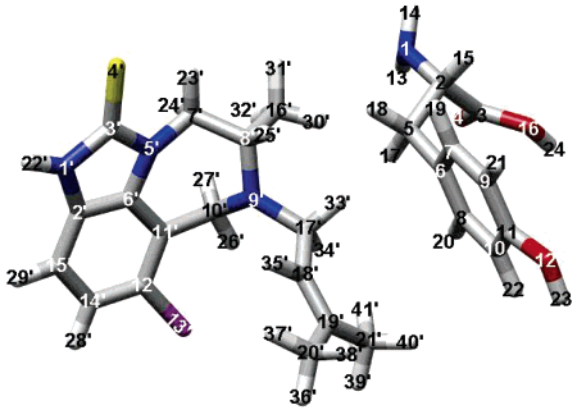

Figure 1. Numbering of atoms for the TIBO/Y181 (C181) dimers: 8 Cl-TIBO/Y181 (W), 8 Cl-TIBO/C181 (M), and 9 Cl-TIBO/Y181. In 9 Cl-TIBO/Y181 dimer, the chlorine atom is in position 14′.

By using the Rasmol[37] software, we obtained the Cartesian coordinates of the inhibitor and of the amino acids of interest. Then hydrogen atoms were added by means of the Babel and Molden softwares.[38,39] From the structures built in the previous stage, we optimized the position of the added atoms. The optimization was carried out by employing the HF/3-21G model. Electron density analysis was accomplished by the NBO, NPA, and AIM methods with the B3LYP/6-31+G(d,p) model.[40] The electron density used for the AIM and NBO analysis was computed by considering only the TIBO and the corresponding amino acid. Calculations were done with Gaussian98,[41] NBO5.0,[42] and AIM2000.[43] Structures were superposed and visualized by means of Chimera.[44]

Results and Discussion

Geometric Analysis. *TIBO/Y181 (C181).* Geometric analysis revealed differences in the analyzed dimers, especially for dihedral angles. The analysis of the superposed structures showed that the main differences lie in the seven-membered ring in the dimethylalyl and methyl substituents of the TIBO inhibitor. The benzimidazole ring was used as reference because the similarity between the dimers is maximum in this ring (Figure 2).

The TIBO dimethylallyl and methyl groups in 9 Cl-TIBO/Y181 dimer are almost in parallel in which the value of the dihedral angle C16′−C8′−N9′−C17′ is 161.4° (Figures 1 and 2). The seven-membered ring is nearly coplanar with the benzimidazole ring.[3] The 8 Cl-TIBO/Y181 (W) and 8 Cl-TIBO/C181 (M) dimers have very similar conformations. Contrary to the structure of 9 Cl-TIBO/Y181 dimer, the seven-membered ring adopts a half-chair conformation in both of these structures, where the dihedral angle C16′−C8′−N9′−C17′ between the methyl and dimethylallyl groups is 70.6° and 81.6° in 8 Cl-TIBO/Y181 (W) and 8 Cl-TIBO/C181 (M) dimers, respectively. Again, the largest deviations occur in both the seven-membered ring and the methyl and dimethylallyl groups. This indicates that the conformation of the inhibitor is heavily dependent on the position of the chlorine atom, making it also dependent on intramolecular interactions. Interactions between the inhibitor

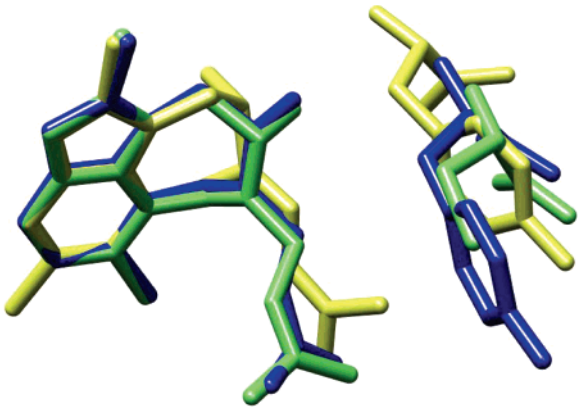

Figure 2. Superposition of 8 Cl-TIBO/Y181 (W) (blue), 8 Cl-TIBO/C181 (M) (green), and 9 Cl-TIBO/Y181 (yellow) dimers.

and amino acids on the binding pocket should alter the preferential conformation only slightly, as it is demonstrated in an analysis of these three isolated TIBO derivatives.[45]

It can be seen that the amino acids superposition is low, especially when the 9 Cl-TIBO/Y181 dimer is compared with the other two complexes. A comparison between 8 Cl-TIBO/Y181 (W) and 9 Cl-TIBO/Y181 dimers shows that the most significant differences lie in the dihedral angles of the atoms in the side chain of Y181 as well as in the hydrogen atoms bound to these atoms. Analysis of the main chain of Y181 and C181 [N1, C2, C3, O4, C5 (C6 in 8 Cl-TIBO/C181 (M) dimer)] of 8 Cl-TIBO/Y181 (W) and 8 Cl-TIBO/C181 (M) dimers gives evidence of the excellent similarity between the geometric parameters.

Conformational analysis of inhibitor TIBO 82913 (1TVR) was carried out in our laboratory by means of the systematic unbounded multiple minimum search (SUMM) method.[46] SUMM is a method for searching internal coordinate conformational space systematically. The search begins at low resolution and then goes to higher and higher resolution because all points in space at a given resolution have been searched.[47] Results showed that the potentially active structure of the inhibitor used in this study is equivalent to the conformer classified as SP5, or the fifth low energy conformation that has a sofa benzodiazepinic ring, and the methyl and dimethylallyl substituents are above the planar part of the molecule. The inhibitors 8 Cl-TIBO studied here can also be classified as SP5, whereas 9 Cl-TIBO does not fit into any of the classes obtained in the reduction stage of the conformational analysis.

TIBO/K101. The superposed structures show that 8 Cl-TIBO/K101 (W) and 8 Cl-TIBO/K101 (M) dimers are very similar, (Figures 3 and 4). On the other hand, the comparison of 8 Cl-TIBO/K101 (W) and 9 Cl-TIBO/K101 indicates that there are outstanding differences in the seven-member ring and in dimethylallyl and methyl substituents of the inhibitor that can be attributed to different positions of chlorine in the TIBO derivatives. Another difference is related to different conformations of K101 in these structures, (Figure 4).

Because of these conformational differences, the sulfur atom (S4′) of the 9 Cl-TIBO/K101 dimer can interact with hydrogens H18 and H19, which is not possible in the case of 8 Cl-TIBO/K101 (W) and 8 Cl-TIBO/K101 (M) dimers. These interactions were analyzed by the NBO and AIM methods and will be further discussed in this work.

TIBO/Y188. Analysis of the geometric parameters of 8 Cl-TIBO/Y188 (W) and 9 Cl-TIBO/Y188 dimers shows that these have very similar bond lengths and bond angles. As for dihedral angles, variations are more significant, especially in the case

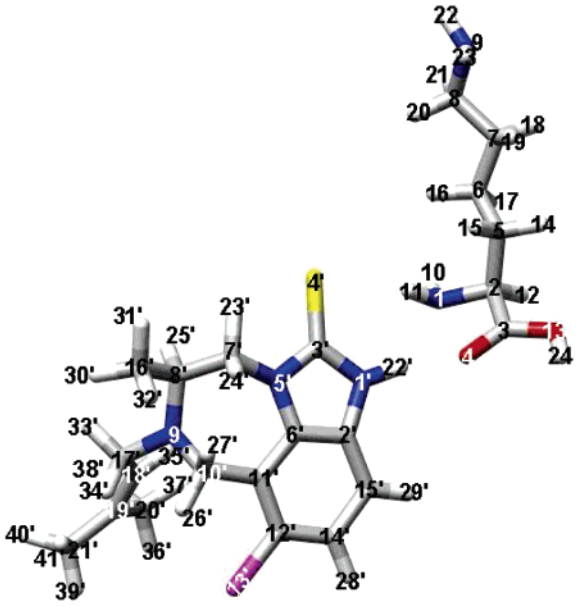

Figure 3. Numbering of atoms for the TIBO/K101dimers: 8 Cl-TIBO/K101 (W), 8 Cl-TIBO/K101 (M), and 9 Cl-TIBO/K101. In 9 Cl-TIBO/K101 dimer, the chlorine atom is in position 14′.

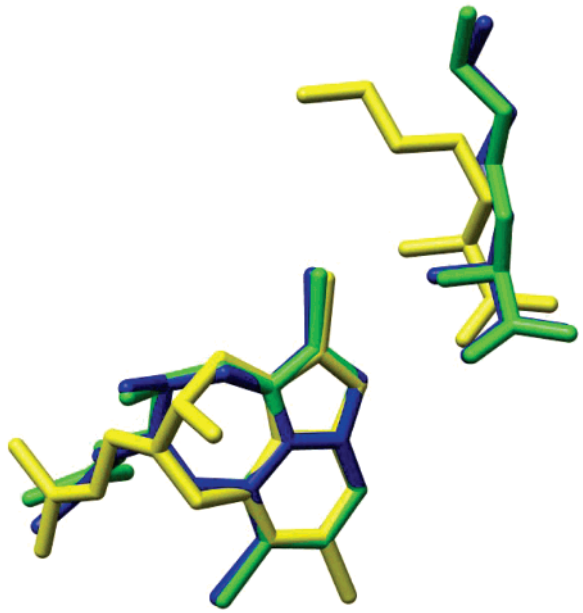

Figure 4. Superposition of the TIBO/K101 dimers: 8 Cl-TIBO/K101 (W) (blue), 8 Cl-TIBO/K101 (M) (green), and 9 Cl-TIBO/K101 (yellow).

of 8 Cl-TIBO/Y188 (W) and 9 Cl-TIBO/Y188 dimers, as can be seen from the superposition of the structures using the inhibitor's benzimidazole as reference (Figures 5 and 6).

Figure 6 also pointed out that the distance between TIBO inhibitor and Y188 (M) in 8 Cl-TIBO/Y188 (M) is the shortest. This closer proximity is possibly related to Y181C mutation, which might lead to a reorientation of the inhibitor. This results in a higher interaction between the inhibitor and Y188 as an attempt to compensate the loss of interactions due to the substitution of Y181 for C181 in the mutant protein.

NBO Analysis. *Second-Order Perturbational Energy ($\Delta E^{(2)}$). TIBO/Y181 (C181)*. The amino acid → TIBO intermolecular interactions in the 8 Cl-TIBO/Y181 (W), 8 Cl-TIBO/Y181 (M), and 9 Cl-TIBO/Y181 dimers are mainly of the $\sigma \rightarrow \sigma^*$ and $n \rightarrow \sigma^*$ type. Interactions of the $\pi \rightarrow \sigma^*$ type are also present

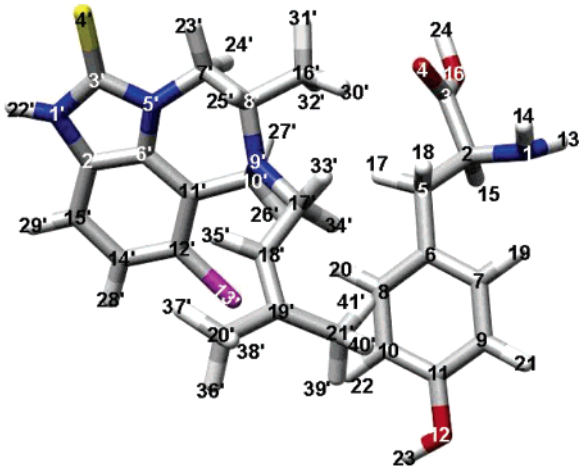

Figure 5. Numbering of atoms for the TIBO/Y188 dimers: 8 Cl-TIBO/Y188 (W), 8 Cl-TIBO/Y188 (M), and 9 Cl-TIBO/Y188. In 9 Cl-TIBO/Y188 dimer, the chlorine atom is in position 14′.

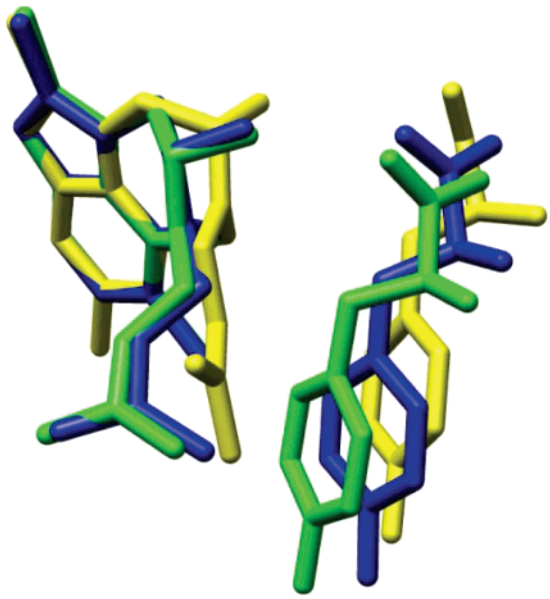

Figure 6. Superposition of the TIBO/amino acid188 dimers: 8 Cl-TIBO/Y188 (W) (blue), 8 Cl-TIBO/Y188 (M) (green), and 9 Cl-TIBO/Y188 (yellow).

in 8 Cl-TIBO/Y181 (W) and 9 Cl-TIBO/Y181 dimers, (Table 1). In the 8 Cl-TIBO/Y181 (W) dimer, most of the interactions occur from σ_{C5-H17} and σ_{C5-H18} to $\sigma^*_{C16'-H30'}$ and $\sigma^*_{C17'-H33'}$ orbitals. The strongest amino acid → TIBO interactions in the 8 Cl-TIBO/Y181 (W), 8 Cl-TIBO/C181 (M), and 9 Cl-TIBO/Y181 dimers are $\sigma_{C5-H17} \rightarrow \sigma^*_{C17'-H33'}$, $\sigma_{C6-H13} \rightarrow \sigma^*_{C17'-H33'}$, and $\pi_{C6-C8} \rightarrow \sigma^*_{C17'-H34'}$, respectively.

The TIBO → amino acid interactions in 8 Cl-TIBO/Y181 (W), 8 Cl-TIBO/C181 (M), and 9 Cl-TIBO/Y181 are mostly of the $\sigma \rightarrow \sigma^*$ type. Interactions of the $n \rightarrow \sigma^*$ and $\sigma \rightarrow \pi^*$ type can also be observed in 9 Cl-TIBO/Y181. The strongest interactions in the 8 Cl-TIBO/Y181 (W), 8 Cl-TIBO/C181 (M), and 9 Cl-TIBO/Y181 dimers are $\sigma_{C17'-H33'} \rightarrow \sigma^*_{C5-H17}$, $\sigma_{C17'-H33'} \rightarrow \sigma^*_{C6-H13}$, and $\sigma_{C21'-H39'} \rightarrow \pi^*_{C10-C11}$, respectively.

The interaction $n_{spN1} \rightarrow \sigma^*_{C16'-H30'}$, present in 8 Cl-TIBO/Y181 (W) and 8 Cl-TIBO/C181 (M) dimers, indicates the occurrence of weak hydrogen bonds of the X−H···A type, where a hydrogen atom forms a bond between the two fragments, both of which or only one of which have low or moderate electronegativity.[48] The analyzed interactions are of the C−H···N type, where a weak donor interacts with a strong acceptor. These interactions have been described in many systems, promoting the stabilization of nitrogen base dimers.[49] In an analysis of RNA structures, various C−H···N contacts were identified between adjacent adenines.[50] These hydrogen bonds also play a key role in crystal engineering.[51]

The sum of electronic stabilization energies, $\sum\Delta E^{(2)}$, for the amino acid → TIBO interactions for the three dimers are equal to 3.70, 1.34, and 2.35 kcal/mol for 8 Cl-TIBO/Y181 (W), 8 Cl-TIBO/C181 (M), and 9 Cl-TIBO/Y181, respectively. For the TIBO → amino acid interactions, the $\sum\Delta E^{(2)}$ values are 1.32, 1.22, and 1.03 kcal/mol for 8 Cl-TIBO/Y181 (W), 8 Cl-TIBO/C181 (M), and 9 Cl-TIBO/Y181 dimers, respectively. These results indicate that: (i) the amino acids are better charge donors than the inhibitors; (ii) the amino acid on 8 Cl-TIBO/Y181 (W) is the one that best donates charge to the inhibitor, while the one that donates the least is the amino acid of 8 Cl-TIBO/C181 (M), possibly because of the loss of interactions due to mutation Y181C; (iii) among the inhibitors studied here, 9 Cl-TIBO is the one that least donates charge. The point (ii) is in accord with the work of Saen-oon et al., who verified that the Y181C mutation eliminates favorable contacts of the aromatic ring of the tyrosine and the bound inhibitor, reducing the stability of TIBO binding.[52]

TIBO/K101. The amino acid → TIBO intermolecular interactions in the 8 Cl-TIBO/K101 (W), 8 Cl-TIBO/K101 (M), and 9 Cl-TIBO/K101 dimers are of the $\sigma \rightarrow \sigma^*$ and $n \rightarrow \sigma^*$ type, (Table 2). In 8 Cl-TIBO/K101 (W) and 8 Cl-TIBO/K101 (M), the acceptor orbital is $\sigma^*_{N1'-H22'}$ in all interactions. In 9 Cl-TIBO/K101, the $\sigma^*_{C3'-S4'}$ orbital also acts as acceptor. This occurs because of the conformational difference displayed by K101 in 9 Cl-TIBO/K101 dimer, which makes the interaction between atoms S4′ and H18 possible. The strongest interactions are $n_{spO4} \rightarrow \sigma^*_{N1'-H22'}$ in 8 Cl-TIBO/K101 (W) and 9 Cl-TIBO/K101, and $n_{pO4} \rightarrow \sigma^*_{N1'-H22'}$ in 8 Cl-TIBO/K101 (M).

The TIBO → amino acid interactions in 8 Cl-TIBO/K101 (W), 8 Cl-TIBO/K101 (M), and 9 Cl-TIBO/K101 are of the $\sigma \rightarrow \sigma^*$ and $n \rightarrow \sigma^*$ type, as well as $n \rightarrow \pi^*$, present in the 8 Cl-TIBO/K101 (W) dimer. Interaction $n_{pS4'} \rightarrow \sigma^*_{N1-H11}$ is the strongest in the three dimers. Interactions $n_{spS4'} \rightarrow \sigma^*_{C7-H18}$, $n_{spS4'} \rightarrow \sigma^*_{C7-H19}$, and $n_{pS4'} \rightarrow \sigma^*_{C7-H19}$ can be observed in 9 Cl-TIBO/K101 only, because only in this one, the amino acid assumes a favorable conformation for these interactions. To date, less attention has been paid to C−H···S interactions because of their rare occurrence in crystals.[53] The studies on intermolecular C−H···S systems are not often reported. Taylor and Kennard in their early study on C−H···X interactions have found only four C−H···S contacts, three of them being intramolecular.[54] However, the significance of this type of interactions in the self-organization of crystals was discussed by Novoa et al.[55] This work shows that C−H···S and C−H···O hydrogen bonds are one of the factors affecting the molecular packing of 1,6-anhydro-2-*O*-(tosyl)-4-*S*-(5,5-dimethyl-2-thioxa-1,3,2-dioxaphosphorinan-2-yl)-*β*-D-glucopyranose molecules in the solid phase. The crystal and electronic structure of (r-2, c-4)-3-benzyl-2,4,5,5-tetraphenyl-1,3-thiazolidine was studied by X-ray crystallography and by theoretical methods.[56] The analysis of geometrical parameters and of bond critical points indicates that C−H···S interactions can be treated as hydrogen bonds. Because the interactions $n_{spS4'} \rightarrow \sigma^*_{C7-H18}$ and $n_{spS4'} \rightarrow \sigma^*_{C7-H19}$ that were observed in the 9 Cl-TIBO/K101 were not confirmed by AIM analysis (see discussion below), we are unsure about making any conclusion regarding the nature of the C−H···S interaction.

TABLE 1: Second-Order Perturbation Energy, $\Delta E^{(2)}$, of the Most Relevant Interactions Taking Place in the TIBO/Y181 (C181) Dimers, (kcal/mol)[a]

8 Cl-TIBO/Y181 (W)		8 Cl-TIBO/C181 (M)		9 Cl-TIBO/Y181	
interaction	$\Delta E^{(2)}$	interaction	$\Delta E^{(2)}$	interaction	$\Delta E^{(2)}$
		Y181 (C181) → TIBO			
$\sigma_{C5-H17} \rightarrow \sigma^*_{C17'-H33'}$	1.31	$\sigma_{C6-H13} \rightarrow \sigma^*_{C17'-H33'}$	0.93	$\pi_{C6-C8} \rightarrow \sigma^*_{C17'-H34'}$	1.00
$\sigma_{C5-H17} \rightarrow \sigma^*_{C16'-H30'}$	1.05	$n_{p\ N\ 1} \rightarrow \sigma^*_{C16'-H30'}$	0.15	$\sigma_{C5-H18} \rightarrow \sigma^*_{C8'-H25'}$	0.64
$n_{sp\ N\ 1} \rightarrow \sigma^*_{C16'-H30'}$	0.53	$\sigma_{C6-H13} \rightarrow \sigma^*_{C16'-H30'}$	0.11	$\sigma_{C5-H17} \rightarrow \sigma^*_{C8'-H25'}$	0.20
$\pi_{C6-C8} \rightarrow \sigma^*_{C17'-H33'}$	0.20	$n_{p\ S7} \rightarrow \sigma^*_{C17'-H33'}$	0.10	$\pi_{C6-C8} \rightarrow \sigma^*_{C21'-H41'}$	0.19
$\sigma_{C5-H18} \rightarrow \sigma^*_{C16'-H30'}$	0.18	$\sigma_{C2-C5} \rightarrow \sigma^*_{C17'-H33'}$	0.05	$\sigma_{C5-H17} \rightarrow \sigma^*_{C17'-H34'}$	0.12
		TIBO → Y181 (C181)			
$\sigma_{C17'-H33'} \rightarrow \sigma^*_{C5-H17}$	0.42	$\sigma_{C17'-H33'} \rightarrow \sigma^*_{C6-H13}$	0.98	$\sigma_{C21'-H39'} \rightarrow \pi^*_{C10-C11}$	0.31
$\sigma_{C17'-H33'} \rightarrow \sigma^*_{C2-C5}$	0.34	$\sigma_{C16'-H30'} \rightarrow \sigma^*_{C6-H13}$	0.18	$\sigma_{C8'-H25'} \rightarrow \sigma^*_{C5-H18}$	0.15
$\sigma_{C16'-H30'} \rightarrow \sigma^*_{C5-C6}$	0.27	$\sigma_{C18'-C19'} \rightarrow \sigma^*_{C6-H13}$	0.06	$n_{p\ N9'} \rightarrow \sigma^*_{C5-H17}$	0.13
$\sigma_{C16'-H30'} \rightarrow \sigma^*_{C5-H17}$	0.24			$\sigma_{C21'-H41'} \rightarrow \pi^*_{C10-C11}$	0.11
$\sigma_{C8'-H25'} \rightarrow \sigma^*_{C5-H18}$	0.05			$\sigma_{C21'-H39'} \rightarrow \sigma^*_{C10-H22}$	0.08

[a] See Figures 1 and S1 (Supporting Information) for details on atom numbering.

TABLE 2: $\Delta E^{(2)}$ of the Most Relevant Interactions Interactions Taking Place in the TIBO/K101 Dimers (kcal/mol)[a]

8 Cl-TIBO/K101 (W)		8 Cl-TIBO/K101 (M)		9 Cl-TIBO/K101	
interaction	$\Delta E^{(2)}$	interaction	$\Delta E^{(2)}$	interaction	$\Delta E^{(2)}$
		K101 → TIBO			
$n_{sp\ O4} \rightarrow \sigma^*_{N1'-H22'}$	17.32	$n_{p\ O4} \rightarrow \sigma^*_{N1'-H22'}$	10.04	$n_{sp\ O4} \rightarrow \sigma^*_{N1'-H22'}$	11.29
$n_{p\ O4} \rightarrow \sigma^*_{N1'-H22'}$	13.19	$n_{sp\ O4} \rightarrow \sigma^*_{N1'-H22'}$	8.87	$n_{p\ O4} \rightarrow \sigma^*_{N1'-H22'}$	3.22
$\sigma_{C3-O4} \rightarrow \sigma^*_{N1'-H22'}$	0.75	$n_{sp\ N1} \rightarrow \sigma^*_{N1'-H22'}$	1.80	$\sigma_{C3-O4} \rightarrow \sigma^*_{N1'-H22'}$	0.16
$n_{sp\ N1} \rightarrow \sigma^*_{N1'-H22'}$	0.47	$\sigma_{C3-O4} \rightarrow \sigma^*_{N1'-H22'}$	0.41	$\sigma_{C7-H18} \rightarrow \sigma^*_{C3'-S4'}$	0.09
$\sigma_{N1-H11} \rightarrow \sigma^*_{N1'-H22'}$	0.29	$\sigma_{N1-H11} \rightarrow \sigma^*_{N1'-H22'}$	0.35	$n_{sp\ N\ 1} \rightarrow \sigma^*_{N1'-H22'}$	0.09
		TIBO → K101			
$n_{p\ S4'} \rightarrow \sigma^*_{N1-H11}$	1.83	$n_{sp\ S4'} \rightarrow \sigma^*_{N1-H11}$	3.14	$n_{p\ S4'} \rightarrow \sigma^*_{N1-H11}$	8.49
$\sigma_{N1'-H22'} \rightarrow \sigma^*_{C3-O4}$	0.54	$n_{sp\ S4'} \rightarrow \sigma^*_{N1-H11}$	0.39	$n_{sp\ S4'} \rightarrow \sigma^*_{N1-H11}$	1.29
$n_{sp\ S4'} \rightarrow \sigma^*_{N1-H11}$	0.17	$n_{sp\ S4'} \rightarrow \sigma^*_{C5-H15}$	0.20	$\sigma_{N1'-H22'} \rightarrow \sigma^*_{C3-O4}$	0.24
$n_{p\ N1'} \rightarrow \pi^*_{C3-O4}$	0.09	$\sigma_{N1'-H22'} \rightarrow \sigma^*_{C3-O4}$	0.15		
$n_{p\ S4'} \rightarrow \sigma^*_{C7-H19}$	0.15	$\sigma_{C3'-S4'} \rightarrow \sigma^*_{N1-H11}$	0.13	$n_{sp\ S4'} \rightarrow \sigma^*_{C7-H18}$	0.11

[a] See Figure 3 for details on atom numbering.

Interactions $n_{pO4} \rightarrow \sigma^*_{N1'-H22'}$ and $n_{spO4} \rightarrow \sigma^*_{N1'-H22'}$, observed in the three dimers, indicate the presence of classic hydrogen bonds, where a hydrogen atom bound to a very electronegative atom is being attracted by another also very electronegative atom. In all three dimers, there is an increase of 0.015−0.017 Å in the N1′−H22′ bond length. These interactions are very strong, as can be seen from the high $\Delta E^{(2)}$ values. Various works report the existence of an N−H···O hydrogen bond between the TIBO inhibitor and K101.[3,4,55,57−59]

Interactions $n_{pS4'} \rightarrow \sigma^*_{N1-H11}$ and $n_{spS4'} \rightarrow \sigma^*_{N1-H11}$ can be considered an indication of hydrogen bonds, though weaker than N−H···O (Figure 7). When substituents in (R_1, R_2)C═S systems are not electron donors, the electronegativity difference between atoms C and S in the C═S bond is close to zero, so hydrogen bond formation is inhibited. However, when $R_1 = R_2 =$ N, as in the case of thiourea and its derivatives, the effective electronegativity of a sulfur atom is significantly increased by resonance effects, which makes this atom an effective acceptor.[60] So hydrogen bonds of the N−H···S type where the sulfur atom takes part in systems of the (R_1, R_2)C═S type are an example of resonance-induced hydrogen bond.[60] Allen et al. observed that the resonance of the $(RNH2)_2$C═S group do not merely assist the hydrogen bond formation, as in a resonance-assisted hydrogen bond, but it is primarily responsible for inducing an accumulation of negative charge on the sulfur.[60] This phenomena is observed in the TIBO/K101 interaction. The TIBO inhibitor presents the (R1, R2)═S (with R1 = R2 = N) system and the strongest intramolecular interactions in this inhibitor are $n_{pN1'} \rightarrow \pi^*_{C3'-S4'}$ and $n_{pN5'} \rightarrow \pi^*_{C3'-S4'}$ (Table S3, Supporting Information), as observed in the isolated 8 and 9 Cl-TIBO.[45] In these interactions, there is strong charge transfer from the lone pairs of N1 and N5 to the π^* orbital of the C3′−S4′ bond, and this transfer becomes even stronger when there is a complexation with the K101. There are various crystallographic studies showing the presence of N−H···S hydrogen bonds in thiourea-derived compounds,[61−68] as well as theoretical studies analyzing

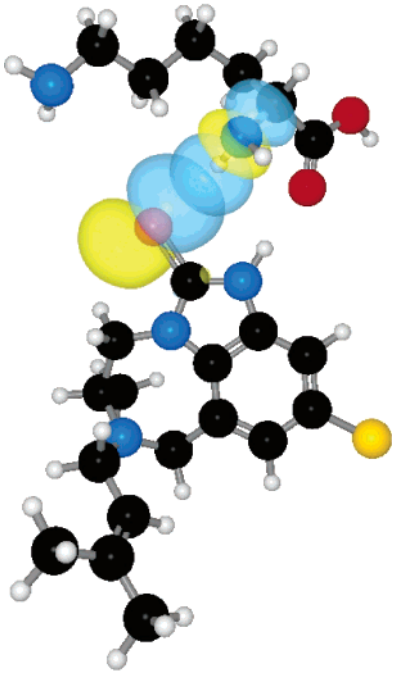

Figure 7. $n_{p\ S4'} \rightarrow \sigma^*_{N1-H11}$. intermolecular interaction in 9 Cl-TIBO/K101 dimer.

TABLE 3: $\Delta E^{(2)}$ of the Most Relevant Interactions Interactions Taking Place in the TIBO/Y188 Dimers, (kcal/mol)[a]

8 Cl-TIBO/Y188 (W)		8 Cl-TIBO/Y188 (M)		9 Cl-TIBO/Y188	
interaction	$\Delta E^{(2)}$	interaction	$\Delta E^{(2)}$	interaction	$\Delta E^{(2)}$
		Y188 → TIBO			
$\pi_{C6-C8} \rightarrow \sigma^*_{C17'-H34'}$	1.63	$\sigma_{C8-H20} \rightarrow \sigma^*_{C10'-H26'}$	3.36	$\pi_{C6-C8} \rightarrow \sigma^*_{C10'-H26'}$	0.45
$\sigma_{C8-H20} \rightarrow \sigma^*_{C10'-H26'}$	1.31	$\pi_{C6-C8} \rightarrow \sigma^*_{C17'-H34'}$	2.63	$\pi_{C3-O4} \rightarrow \sigma^*_{C16'-H30'}$	0.36
$\pi_{C6-C8} \rightarrow \sigma^*_{C21'-H41'}$	0.87	$\sigma_{C5-H17} \rightarrow \sigma^*_{C17'-H34'}$	1.00	$\sigma_{C5-H17} \rightarrow \sigma^*_{C16'-H30'}$	0.33
$\sigma_{C8-H20} \rightarrow \sigma^*_{C17'-H34'}$	0.37	$n_{sp\ O4} \rightarrow \sigma^*_{C16'-H30'}$	1.00	$\sigma_{C8-H20} \rightarrow \sigma^*_{C10'-H26'}$	0.21
$\pi_{C3-O4} \rightarrow \sigma^*_{C16'-H32'}$	0.34	$\pi_{C3-O4} \rightarrow \sigma^*_{C16'-H30'}$	0.50	$\sigma_{C5-H17} \rightarrow \sigma^*_{C10'-H27'}$	0.11
$n_{sp\ O4} \rightarrow \sigma^*_{C16'-H32'}$	0.17	$n_{sp\ O4} \rightarrow \sigma^*_{C8'-C16'}$	0.44	$n_{p\ O4} \rightarrow \sigma^*_{C16'-H30'}$	0.05
		TIBO → Y188			
$n_{p\ Cl13'} \rightarrow \sigma^*_{C8-H20}$	1.54	$\sigma_{C10'-H26'} \rightarrow \sigma^*_{C8-H20}$	2.51	$\sigma_{C16'-H30'} \rightarrow \sigma^*_{C5-H17}$	0.23
$\sigma_{C10'-H26'} \rightarrow \sigma^*_{C8-H20}$	1.00	$n_{p1\ Cl13'} \rightarrow \sigma^*_{C8-H20}$	1.06	$\sigma_{C10'-H26'} \rightarrow \sigma^*_{C5-H17}$	0.21
$n_{sp\ Cl13'} \rightarrow \sigma^*_{C8-H20}$	0.36	$\sigma_{C17'-H34'} \rightarrow \sigma^*_{C2-C5}$	0.90	$\sigma_{C10'-H27'} \rightarrow \pi^*_{C6-C8}$	0.07
$\sigma_{C17'-H34'} \rightarrow \sigma^*_{C2-C5}$	0.20	$\sigma_{C16'-H30'} \rightarrow \pi^*_{C3-O4}$	0.48	$\sigma_{C16'-H32'} \rightarrow \pi^*_{C3-O4}$	0.16
$n_{sp\ Cl13'} \rightarrow \sigma^*_{C10-H22}$	0.30				

[a] See Figure 5 for details on atom numbering.

the ability of the sulfur atom to act as proton acceptor.[69−72] Nevertheless, this is the first time that the presence of the hydrogen bond is reported to be involved in the stabilization of the TIBO inhibitor with K101.

The sum of the stabilization energies of the amino acid → TIBO interactions gives values of 32.02, 21.59, and 14.94 kcal/mol for 8 Cl-TIBO/K101 (W), 8 Cl-TIBO/K101 (M), and 9 Cl-TIBO/K101 dimers, respectively. The sum of the stabilization energies of the TIBO → amino acid interactions leads to values of 2.63, 4.12, and 10.38 kcal/mol for 8 Cl-TIBO/K101 (W), 8 Cl-TIBO/K101 (M), and 9 Cl-TIBO/K101, respectively. According to these results, it is possible to state that (i) in all the dimers, K101 is the one who donates charge to the TIBO inhibitor, (ii) the amino acid in 8 Cl-TIBO/K101 (W) is the one that most donates charge to the inhibitor, followed by 8 Cl-TIBO/K101 (M) and 9 Cl-TIBO/K101, and (iii) the inhibitor that most donates charge is 9 Cl-TIBO.

TIBO/Y188. The amino acid → TIBO intermolecular interactions in 8 Cl-TIBO/Y188 (W), 8 Cl-TIBO/Y188 (M), and 9 Cl-TIBO/Y188 dimers are of the $\pi \rightarrow \sigma^*$, $\sigma \rightarrow \sigma^*$, and $n \rightarrow \sigma^*$ type (Table 3). In 8 Cl-TIBO/Y188 (W) and 8 Cl-TIBO/Y188 (M), the main acceptor orbitals are $\sigma^*_{C17'-H34'}$ and $\sigma^*_{C10'-H26'}$. The strongest interactions in 8 Cl-TIBO/Y188 (W), 8 Cl-TIBO/Y188 (M), and 9 Cl-TIBO/Y188 dimers are $\pi_{C6-C8} \rightarrow \sigma^*_{C17'-H34'}$, $\sigma_{C8-H20} \rightarrow \sigma^*_{C10'-H26'}$, and $\pi_{C6-C8} \rightarrow \sigma^*_{C10'-H26'}$, respectively.

The main TIBO → amino acid interactions in 8 Cl-TIBO/Y188 (W), 8 Cl-TIBO/Y188 (M), and 9 Cl-TIBO/Y188 are of the $\sigma \rightarrow \sigma^*$, $\sigma \rightarrow \pi^*$, and $n \rightarrow \sigma^*$ type. The strongest interactions in 8 Cl-TIBO/Y188 (W), 8 Cl-TIBO/Y188 (M), and 9 Cl-TIBO/Y188 are $n_{pCl13'} \rightarrow \sigma^*_{C8-H20}$, $\sigma_{C10'-H26'} \rightarrow \sigma^*_{C8-H20}$, and $\sigma_{C16'-H30'} \rightarrow \sigma^*_{C5-H17}$, respectively.

The number of amino acid → TIBO and TIBO → amino acid interactions observed in 8 Cl-TIBO/Y188 (M) was much higher than those observed for 8 Cl-TIBO/Y188 (W) and 9 Cl-TIBO/Y188. Figure 6 shows that the inhibitor is closer to the amino acid in the 8 Cl-TIBO/Y188 (M) dimer than in the others. So more interactions occur in 8 Cl-TIBO/Y188 (M) and they have higher stabilization energies. This closer proximity between the inhibitor and the amino acid in 8 Cl-TIBO/Y188 (M) dimer is probably related to the Y181C mutation, which causes a reorientation of the inhibitor, increasing its interactions with Y188 in an attempt to partially compensate the loss of the favorable interactions upon mutation.

The $n_{spO4} \rightarrow \sigma^*_{C16'-H30'}$ and $n_{spO4} \rightarrow \sigma^*_{C16'-H32'}$ interactions can be considered an indication of weak hydrogen bonds of the C−H···O type. Various evidence supports the existence of this hydrogen bond, including its presence in the interior and in the interface of proteins.[54,73−78] Some studies have suggested that hydrogen bonds of this type significantly contribute to protein−inhibitor interactions.[76,77]

TABLE 4: NPA Charges Exhibiting the Widest Variations among the TIBO/Y181 (C181) Dimers[a]

8 Cl-TIBO/Y181 (W)		8 Cl-TIBO/C181 (M)		9 Cl-TIBO/Y181	
atom	charge	atom	charge	atom	charge
		TIBO			
C12′	−0.062			C12′	−0.248
Cl13	0.010			C13	−0.084
C14	−0.248			Cl14	0.036

[a] See Figures 1 and S1 (Supporting Information) for details on atom numbering.

The $\sum \Delta E^{(2)}$ values of the amino acid → TIBO interactions in the three dimers are equal to 6.00, 12.43, and 1.73 kcal/mol for 8 Cl-TIBO/Y188 (W), 8 Cl-TIBO/Y188 (M), and 9 Cl-TIBO/Y188, respectively. For the TIBO → amino acid interactions, the $\sum \Delta E^{(2)}$ values are equal to 4.19, 7.65, and 0.51 kcal/mol for 8 Cl-TIBO/Y188 (W), 8 Cl-TIBO/Y188 (M), and 9 Cl-TIBO/Y188, respectively. These results show that (i) Y188 donates charge to the TIBO inhibitor in all dimers, (ii) the amino acid in 8 Cl-TIBO/Y188 (M) is the one that most donates charge to the inhibitor, followed by the amino acid in 8 Cl-TIBO/Y188 (W), and 9 Cl-TIBO/Y188, and (iii) 8 Cl-TIBO is the inhibitor that most donates charge.

Natural Population Analysis. *TIBO/Y181 (C181).* The natural atomic charges of 8 Cl-TIBO/Y181 (W) and 8 Cl-TIBO/C181 (M) obtained by the NPA method are very similar. There is a slightly wider variation by comparing the 8 Cl-TIBO/Y181 (W) and 9 Cl-TIBO/Y181. The most significant variations occurred between atoms C12′, C113′, and C14′ in 8 Cl-TIBO/Y181 (W) and atoms C12′, C13′, and Cl14′ in 9 Cl-TIBO/Y181 dimer (Table 4). These variations are due to the different positions of the chlorine atom, and to the different conformations between 8 Cl-TIBO/Y181 (W) and 9 Cl-TIBO/Y181.

In all dimers, the amino acid → TIBO charge transfer is equal to 7.58, 4.65, and 2.79×10^{-3} e in 8 Cl-TIBO/Y181 (W), 8 Cl-TIBO/C181 (M), and 9 Cl-TIBO/Y181, respectively. NPA data agree with the second-order stabilization energies ($\Delta E^{(2)}$) and: (i) in all cases, the amino acid donates charge to the inhibitor, (ii) the strongest charge transfer occurs in 8 Cl-TIBO/Y181 (W), followed by 8 Cl-TIBO/C181 (M) and 9 Cl-TIBO/Y181, respectively, and (iii) charge transfer is stronger in 8 Cl-TIBO/Y181 (W) than in 8 Cl-TIBO/C181 (M).

From item (ii), it can be seen that, despite the mutation, the amino acid−TIBO interaction is more effective in 8 Cl-TIBO/

TABLE 5: NPA Charges Exhibiting the Widest Variations among the TIBO/Y188 Dimers[a]

8 Cl-TIBO/Y188 (W)		8 Cl-TIBO/Y188 (M)		9 Cl-TIBO/Y188	
atom	charge	atom	charge	atom	charge
		Y188			
N1	−0.920			N1	−0.934
C3	0.800			C3	0.819
C6	−0.080			C6	−0.068
C8	−0.217	C8	−0.203	C8	−0.221
H19	0.263			H19	0.244
		TIBO			
N1′	−0.610			N1′	−0.575
C2′	0.129			C2′	0.163
S4′	−0.212	S4′	−0.222	S4′	−0.263
C11′	−0.032			C11′	−0.054
C12′	−0.054	C12′	−0.065	C12′	−0.251
C15′	−0.251			C15′	−0.286
C16′	−0.695			C16′	−0.718
C18′	−0.238			C18′	−0.251
C19′	−0.037			C19′	−0.011
C21′	−0.699			C21′	−0.714
H23′	0.300			H23′	0.257
H24′	0.245			H24′	0.275
H27′	0.223			H27′	0.256
H30′	0.246	H30′	0.259	H30′	0.252
H31′	0.236			H31′	0.261
H32′	0.236	H32′	0.223		

[a] See Figure 5 for details on atom numbering.

C181 (M) dimer than in 9 Cl-TIBO/Y181. Item (iii) can be considered a possible cause of inhibitor activity loss due to mutation Y181C because of the loss of favorable interactions between TIBO and Y181.[3,27]

TIBO/K101. The natural atomic charges in 8 Cl-TIBO/K101 (W) and 8 Cl-TIBO/K101 (M) are very similar. The conformational difference observed in the amino acid and in the inhibitor of 9 Cl-TIBO/K101 when compared with 8 Cl-TIBO/K101 (W) and 8 Cl-TIBO/K101 (M) results in wider variation of the NPA charges of the former dimer when compared with the latter two.

In 8 Cl-TIBO/K101 (W) and 8 Cl-TIBO/K101 (M) was verified an amino acid → TIBO charge transfer of the 37.62 and 24.49 × 10^{-3} e, respectively. As for 9 Cl-TIBO/K101, a TIBO → amino acid charge transfer equal to 3.19 × 10^{-3} e was observed. These results agree with results from the second-order energetic analysis, which showed that the strongest charge transfer occurs in 8 Cl-TIBO/K101 (W), followed by 8 Cl-TIBO/K101 (M). This indicates that mutation also affects interaction of the inhibitors with amino acids located away from the mutation point. Contrary to 8 Cl-TIBO/K101 (W) and 8 Cl-TIBO/K101 (M), the inhibitor in 9 Cl-TIBO/K101 donates charge to the amino acid, which is also in agreement with the second-order energetic analysis.

TIBO/Y188. There is close similarity between the NPA charges of the atoms of 8 Cl-TIBO/Y188 (W) and 8 Cl-TIBO/Y188 (M). The widest variations occurred in the C8 atom in the amino acid and in S4′, C12′, H30′, and H32′ atoms in the inhibitor (Table 5). Great similarity is also observed between the NPA charges of the atoms of 8 Cl-TIBO/Y188 (W) and 9 Cl-TIBO/Y188. The most significant variations are observed for N1, C3, C6, H17, and H19 atoms in the amino acid and N1′, C2′, S4′, C11′, C12′, C15′, C16′, C18′, C19′, C21′, H23′, H24′, H27′, and H31′ atoms in the inhibitor. As previously discussed, these wider variations are related to the different positions of the chlorine atoms in 8 Cl-TIBO and 9 Cl-TIBO as well as to differences in conformations observed between these inhibitors.

TABLE 6: Bond Properties of the Intermolecular Interactions in the 8 Cl-TIBO/Y181 (W) Dimer[a]

	interaction	$\rho_b(r)$	$L(r)$	ϵ	RCP−BCP	$\rho_r(r)$[b]
1	N1···H30′	0.007	−0.006	0.336	0.393	0.007
2	H17···H30′	0.013	−0.013	0.929	0.762	0.008
3	H17···H33′	0.016	−0.014	0.249	0.809	0.008
4	C8···H40′	0.003	−0.002	2.482	1.069	0.003

[a] $\rho(r)$ and $L(r)$ in au, BCP−RCP in Å. See Figure 1 for details on atom numbering. [b] Electron density in the nearest RCP from the corresponding BCP, indicated in Figure 8 by capital letters.

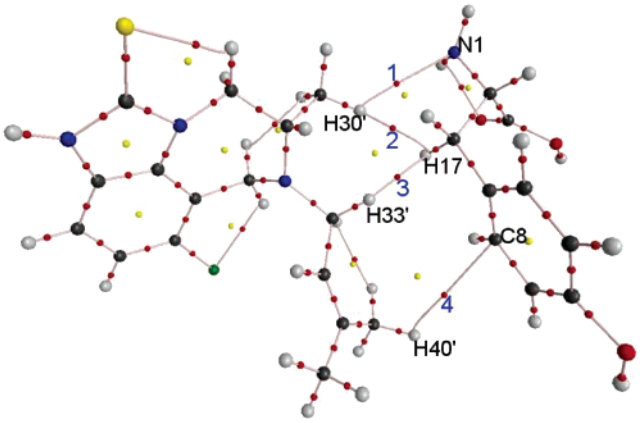

Figure 8. Molecular graph for 8 Cl-TIBO/Y181 (W) dimer. (1) N1···H30′; (2) H17···H30′; (3) H17···H33′; (4) C8···H40′.

An amino acid → TIBO charge transfer of the 1.86, 3.68, and 2.99 × 10^{-3} e was observed in the 8 Cl-TIBO/Y188 (W), 8 Cl-TIBO/Y188 (M), and 9 Cl-TIBO/Y188 dimers, respectively. These data show that the strongest charge transfer takes place in 8 Cl-TIBO/Y188 (M) dimer, which agrees with results from the second-order energetic analysis. Charge transfer is stronger in 9 Cl-TIBO/Y188 dimer than in 8 Cl-TIBO/Y188 (W) dimer, a result that does not agree with the second-order stabilization energetic analysis.

Atoms in Molecules. *Analysis of the Properties at the Critical Points. TIBO/Y181 (C181).* Four intermolecular bond critical points (BCPs) can be located in the 8 Cl-TIBO/Y181 (W) dimer (Table 6 and Figure 8). The BCPs **1**−**4** satisfy the criteria proposed by Popelier[79] for the characterization of hydrogen bonds. Interaction **1** can be considered a weak hydrogen bond. Bader and Matta observed the formation of four interactions of the C−H···N type in amino acid leucine, where $\rho_b(r)$ falls within 0.007−0.011 au.[80] The other three interactions are traditionally considered as steric repulsions, even using AIM,[81] but Matta et al. proved that the presence of a bond path between hydrogens bearing the same charge in some hydrocarbons makes a stabilizing contribution, the so-called hydrogen−hydrogen bond, or H···H bond.[82] By analogy, it is possible to suppose that the existence of a bond path, BP, between nonbonded carbon and hydrogen originates an attractive C···H bond. Some important parameters for the description of this interaction are the difference between the electronic densities at the BCP, $\rho_b(r)$, and at the ring critical point (RCP), $\rho_r(r)$, the ellipticity at BCP value, ϵ, as well as the distance between the BCP and the ring critical point, RCP. All three parameters indicate how stable the system is through small variations in geometries. High ϵ, small BCP−RCP distance and the near equality of ρ_b and ρ_r, and a curved bond path, BP, shows that the interaction is structurally unstable, or labile, because the BCP may be destroyed upon binding to the RCP.[35,82,83] All BPs containing the four BCPs are curved, despite the fact that the difference between the bond path length, BPL, and the bond length, BL,

TABLE 7: Bond Properties of the Intermolecular Interactions in the 8 Cl-TIBO/C181 (M) Dimer[a]

	interaction	$\rho_b(r)$	$L(r)$	ϵ	RCP−BCP	$\rho_r(r)$[b]
1	N1···H30′	0.003	−0.002	0.325	0.445	0.003
2	H13···H30′	0.004	−0.003	0.503	0.397	0.004
3	H13···H33′	0.011	−0.009	0.053	1.009	0.004
4	S7···H40′	0.001	−0.001	0.384	0.903	0.009

[a] $\rho(r)$ and $L(r)$ in au, BCP−RCP in Å. See Figure S1 (Supporting Information) for details on atom numbering. [b] Electron density in the nearest RCP from the corresponding BCP, indicated in Figure S2 (Supporting Information) by capital letters.

TABLE 8: Bond Properties of the Intermolecular Interactions in the 9 Cl-TIBO/Y181 Dimer[a]

	interaction	$\rho_b(r)$	$L(r)$	ϵ	RCP−BCP	$\rho_r(r)$[b]
1	BCP···H25′	0.008	−0.007	3.287	1.199	0.004
2	C6···H34′	0.007	−0.005	1.364	0.919	0.004
3	C10···H41′	0.008	−0.007	1.680	2.104	0.004

[a] $\rho(r)$ and $L(r)$ in au, BCP−RCP in Å. See Figure 1 for details on atom numbering. [b] Electron density in the nearest RCP from the corresponding BCP, indicated in Figure S3 (Supporting Information) by capital letters.

is large only for **2**. BCPs **2** and **4** have very high ellipticities, and for **1** and **4** $\rho_b(r)$ is equal to $\rho_r(r)$. The only small BCP−RCP distance is for interaction **1**. These data can indicate that these interactions are unstable, or at least not very stable, but the existence of a bond path indicates that **2** and **3** (H···H) and **4** (C···H) are bonds that stabilize the dimer. It is interesting to note that both H···H bonds fit all criteria proposed by Matta et al.[82]

Four BCPs can also be observed in 8 Cl-TIBO/C181 (M) dimer (Table 7 and Figure S2, Supporting Information). Interactions **1**−**3** satisfy Popelier's criteria. All present small ϵ and linear BP, but BCP−RCP is small and $\rho_b \approx \rho_r$ for **1** and **2**, which indicates that these two are not very stable. **1** can be seen as a weak hydrogen bond of the C−H···N type, and **2** and **3** are H···H bonds. **4** can be considered a weak C−H···S bond, despite its $\rho_b(r)$ being below the proposed range, and the BP is curved but its BCP−RCP distance is long, and $\rho_r(r)$ is very different from $\rho_b(r)$. The BCPs N1···H30′, H13···H30′, and H13···H33′ in 8 Cl-TIBO/C181 (M) are equivalent to BCPs N1···H30′, H17···H30′, and H17···H33′ in 8 Cl-TIBO/Y181 (W). However, $\rho_r(r)$ values for these interactions are higher in the latter than in the former. Because the density at the BCP is an indication of the bond strength,[35] these results give evidence that the amino acid−inhibitor interaction is stronger in 8 Cl-TIBO/Y181 (W) than in 8 Cl-TIBO/C181 (M).

Three intermolecular BCPs can be observed in 9 Cl-TIBO/Y181 dimer (Table 8 and Figure S3, Supporting Information). These interactions are very weak and unstable because they have high ellipticity, their BP are highly curved despite their relatively long BCP−RCP distances, and ρ_b is very different from ρ_r. BCP **1** is interesting because it is not located between two atoms but between an atom and another BCP. When a BCP is generated from the union of a nucleus and another BCP, a *conflict mechanism* takes place.[79] This phenomenon occurs because the nucleus cannot decide between the two nuclei bound to the BCP. The two acceptor nuclei compete for the "indecisive" nucleus. Infinitesimal geometric variations are enough for a conflict structure to turn into the other one. A feature of a conflict structure is that all the critical points are stable, while the molecular graph itself is unstable.[79] Therefore, upon slight variations in the geometry of the dimer, BCP **1** will bind to either C5 or H18. BCPs **2** and **3** indicate C···H bonds.

TABLE 9: Bond Properties of the Intermolecular Interactions in the 8 Cl-TIBO/K101 (W) Dimer[a]

	interaction	$\rho_b(r)$	$L(r)$	ϵ	RCP−BCP	$\rho_r(r)$[b]
1	O4···H22′	0.044	−0.040	0.036	1.589	0.003
2	S4′···H11	0.005	−0.004	0.024	0.830	0.003

[a] $\rho(r)$ and $L(r)$ in au, BCP−RCP in Å. See Figure 3 for details on atom numbering. [b] Electron density in the nearest RCP from the corresponding BCP, indicated in Figure 9 by capital letters.

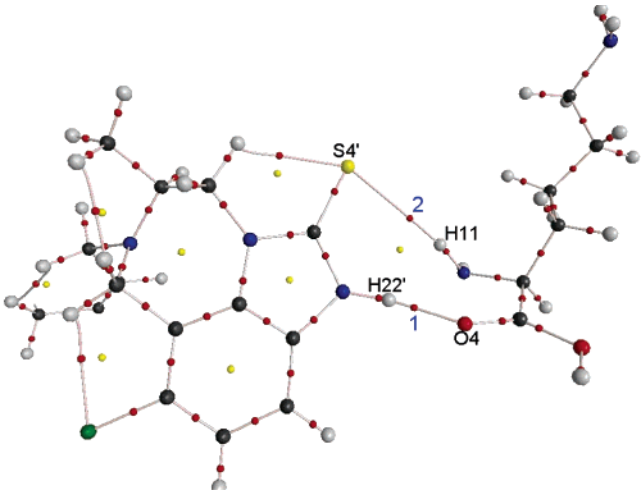

Figure 9. Molecular graph for 8 Cl-TIBO/K101 (W) dimer: (1) O4···H22′; (2) S4′···H11.

Results from the AIM analysis indicate: (i) the presence of the interactions of C−H···N weak hydrogen bonds between 8 Cl-TIBO and Y181 and C181, thus confirming the results from the NBO analysis. This type interaction is not observed in 9 Cl-TIBO/Y181 in AIM or NBO: (ii) in agreement with the NBO, the AIM analysis showed that the stabilization of the dimers is mainly due to van der Waals hydrophobic interactions between the inhibitor and the amino acids as C···H and H···H bonds. The nature of the amino acid−TIBO interactions are in agreement with experimental data, indicating that the allosteric pocket where the NNRTIs form complexes with the enzyme is hydrophobic.[3,27]

TIBO/K101. Two intermolecular interactions were observed in 8 Cl-TIBO/K101 (W) dimer: O4···H22′ and S4′···H11 (Table 9 and Figure 9). Interaction **1** is a typical hydrogen bond, which presents a decrease in the electron density (from 0.352 au in the monomer to 0.335 au in the dimer). Also, both the density and the Laplacian fall within the range proposed by Popelier.[79] Interaction **2** can also be considered a hydrogen bond of the N−H···S type because there is an increase in the N1−H11 bond length of 0.006 Å with dimerization and a decrease of the electron density at the BCP (0.351 au in the monomer against 0.348 au in the dimer), thus indicating weakening of this bond. In addition, the noncurved bond path, the long BCP−RCP distance, and the low ellipticity indicate that the bond is stable.[81,82] For this interaction, both $\rho_b(r)$ and $L(r)$ fall within the range proposed for a hydrogen bond.[79] However, this interaction is weaker than interaction O4···H22′, as judged from its lower $\rho_b(r)$ value. This fact is possibly related to both the lower electronegativity of the sulfur atom and the longer S4′···H11 intermolecular distance. In the literature, there are some works reporting that, according to the AIM method, interactions of the N−H···S and O−H···S type have all the features of a hydrogen bond.[69,71,72,83]

Intermolecular interactions O4···H22′ and S4′···H11 were also observed in 8 Cl-TIBO/K101 (M) dimer (Table 10 and

TABLE 10: Bond Properties of the Intermolecular Interactions in the 8 Cl-TIBO/K101 (M) Dimer[a]

	interaction	$\rho_b(r)$	$L(r)$	ϵ	RCP−BCP	$\rho_r(r)$[b]
1	O4···H22′	0.033	−0.028	0.047	1.595	0.004
2	S4′···H11	0.008	−0.006	0.010	0.912	0.004

[a] $\rho(r)$ and $L(r)$ in au, BCP−RCP in Å. See Figure 3 for details on atom numbering. [b] Electron density in the nearest RCP from the corresponding BCP, indicated in Figure S4 (Supporting Information) by capital letters.

TABLE 11: Bond Properties of the Intermolecular Interactions in the 9 Cl-TIBO/K101 Dimer[a]

	interaction	$\rho_b(r)$	$L(r)$	ϵ	RCP−BCP	$\rho_r(r)$[b]
1	O4···H22′	0.024	−0.020	0.047	1.214	0.004
2	S4′···H11	0.016	−0.010	0.010	1.201	0.004

[a] $\rho(r)$ and $L(r)$ in au, BCP−RCP in Å. See Figure 3 for details about atom numbering. [b] Electron density in the nearest RCP from the corresponding BCP, indicated in Figure S5 (Supporting Information) by capital letters.

Figure S4, Supporting Information). The former interaction is a hydrogen bond because it takes place between a strong proton acceptor (C═O) and a strong proton donor (N−H) and the fact that the electron density and the Laplacian fall within the range proposed by Popelier.[79] Interaction **1** is weaker in 8 Cl-TIBO/K101 (M) when compared with 8 Cl-TIBO/K101 (W) because of the lower $\rho_b(r)$ value in the former. This fact may be related to the longer O4···H22′ distance in 8 Cl-TIBO/K101 (M) dimer. **2** can also be described as a hydrogen bond, although it is weaker than **1**. Facts supporting this hypothesis are the lowering of the electron density at the BCP, (from 0.351 au in the monomer to 0.348 au in the dimer), which indicates weakening of this bond and the value of $\rho_b(r)$ and $L(r)$, which are characteristic of hydrogen bonds. The noncurved bond path, a high BCP−RCP distance, the large difference between $\rho_b(r)$ and $\rho_r(r)$, and the low ellipticity indicate that this interaction is stable.

As in the case of the two former dimers, two intermolecular interactions are also observed for 9 Cl-TIBO/K101 (Table 11 and Figure S5, Supporting Information). **1** (O4···H22′) is a hydrogen bond because it satisfies the criteria proposed by Popelier. Moreover, this interaction involves a strong proton acceptor and a strong proton donor. **2** (S4′···H11) can also be treated as a hydrogen bond, although weaker than interaction **1**, and satisfies Popelier criteria. It is stronger in 9 Cl-TIBO/K101 than those observed for 8 Cl-TIBO/K101 (W) and 8 Cl-TIBO/K101 (M) because the density at the S4′···H11 BCP is the highest. Both present linear bond paths, long BCP−RCP distances, low ellipticities, and $\rho_b(r)$ is different from $\rho_r(r)$, which indicate that these interactions are stable.

Results from the AIM analysis show that the dimers are not only stabilized by hydrogen bond O4···H22′, but also by S4′···H11, which are in agreement with the NBO analysis. The last hydrogen bond had not yet been described for the RT/TIBO system in the literature.

TIBO/Y188. Eight intermolecular BCPs can be observed in the 8 Cl-TIBO/Y188 (W) dimer (Table 12 Figure 10). All the BCPs have $\rho_b(r)$ and $L(r)$ values falling in the range proposed by Popelier for the characterization of a hydrogen bond.[79] The BCP−RCP distances are small for **2**, **4**, and **6**, their BPs are curved, and $\rho_b = \rho_r$. It can be concluded that these BPs are unstable. In addition, interactions **6**−**8** have the highest ellipticities among all the intermolecular interactions, which indicates that these interactions are also unstable and weak.[35,83−85] The only interaction that can be treated as a hydrogen bond (though

TABLE 12: Bond Properties of the Intermolecular Interactions in the 8 Cl-TIBO/Y188 (W) Dimer[a]

	interaction	$\rho_b(r)$	$L(r)$	ϵ	RCP−BCP	$\rho_r(r)$[b]
1	H20···Cl13′	0.010	−0.009	0.084	0.431	0.009
2	H17···H26′	0.005	−0.005	0.521	0.525	0.005
3	H20···H26′	0.012	−0.010	0.119	0.603	0.009
4	H18···H30′	0.003	−0.003	0.750	0.210	0.003
5	O4···H32′	0.010	−0.009	0.341	1.128	0.003
6	H17···H32′	0.003	−0.003	1.416	0.125	0.003
7	C8···H34′	0.011	−0.009	1.033	0.790	0.007
8	C8···H41′	0.009	−0.007	1.192	0.691	0.007

[a] $\rho(r)$ and $L(r)$ in au, BCP−RCP in Å. See Figure 5 for details on atom numbering. [b] Electron density in the nearest RCP from the corresponding BCP, indicated in Figure 10 by capital letters.

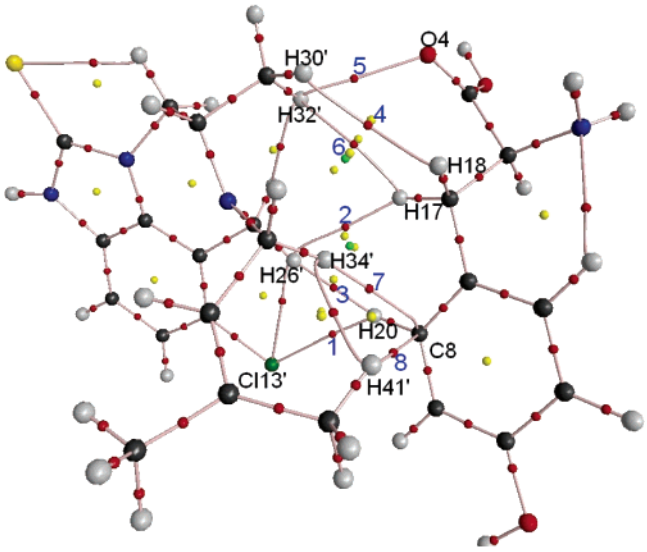

Figure 10. Molecular graph for 8 Cl-TIBO/Y188 (W) dimer: (1) H20···Cl13′; (2) H17···H26′; (3) H20···H26′; (4) H18···H30′; (5) O4···H32′; (6) H17···H32′; (7) C8···H34′; (8) C8···H41′.

weak) is O4···H32′, which has low ellipticity and long BCP−RCP distance. **2**−**4** and **6** can be considered stabilizing H···H bonds, and **7** and **8** are C···H bonds. Interaction **1** is an interesting case because it occurs between Cl13′ and H20 atoms. To date, there is no consensus on whether interactions of the C−H···Cl type are hydrogen bonds. Apparently, interactions of the C−H···Cl$^-$ and C−H···Cl−M (M = metal) types can be considered hydrogen bonds, whereas C−H···Cl−C interactions would hardly be taken as such without activation of the acceptor via formation of an anion or by coordination to a metal.[86] Nevertheless, C−H···Cl interactions have been shown to be of great importance in several areas such as molecular recognition, reactivity, and structure of biochemical species, stability of metal complexes, crystal engineering, and determination of molecular conformations.[87−90]

Eight intermolecular BCPs can be observed also in the 8 Cl-TIBO/Y188 (M) dimer (Table 13 and Figure S6, Supporting Information). BCPs **6**−**8** also have higher ellipticity values, and their BPs are curved despite their long BCP−RCP distances, which indicate that these interactions are weak and unstable, so any geometric distortion may promote their cleavage. These interactions are attractive C···H bonds. Also, the BP is curved for **2** and **5**, indicating that these interactions can be unstable. Although the $\rho_b(r)$ and $L(r)$ values of BCPs **1**−**8** fall within the range proposed for the establishment of a hydrogen bond,[77] only the interaction O4···H30′ can be considered a weak hydrogen bond because it has low ellipticity and a reasonable BCP−RCP.

TABLE 13: Bond Properties of the Intermolecular Interactions in the 8 Cl-TIBO/Y188 (M) Dimer[a]

	interaction	$\rho_b(r)$	$L(r)$	ϵ	RCP−BCP	$\rho_r(r)$[b]
1	Cl13′···H22	0.011	−0.010	0.591	0.274	0.010
2	Cl13′···H20	0.006	−0.006	0.374	0.480	0.005
3	H20···H26′	0.022	−0.014	0.034	0.779	0.008
4	O4···H30′	0.018	−0.017	0.229	0.999	0.006
5	H17···H30′	0.007	−0.006	0.659	0.333	0.006
6	C5···H34′	0.020	−0.021	1.083	1.516	0.006
7	C6···H40′	0.010	−0.008	1.831	1.249	0.007
8	C11···H41′	0.006	−0.005	1.389	1.063	0.004

[a] $\rho(r)$ and $L(r)$ in au, BCP−RCP in Å. See Figure 5 for details about atom numbering. [b] Electron density in the nearest RCP from the corresponding BCP, indicated in Figure S6 (Supporting Information) by capital letters.

TABLE 14: Bond Properties of the Intermolecular Interactions in the 9 Cl-TIBO/Y188 Dimer[a]

	interaction	$\rho_b(r)$	$L(r)$	ϵ	RCP−BCP	$\rho_r(r)$[b]
1	C8···H26′	0.006	−0.005	0.608	0.796	0.004
2	H17···H27′	0.006	−0.006	0.658	0.608	0.005
3	O4···H30′	0.004	−0.004	0.219	0.696	0.003
4	H17···H30′	0.006	−0.005	0.224	0.564	0.005
5	C11···H38′	0.004	−0.003	1.903	1.130	0.002

[a] $\rho(r)$ and L(r) in au, BCP−RCP in Å. See Figure 5 for details on atom numbering. [b] Electron density in the nearest RCP from the corresponding BCP, indicated in Figure S7 (Supporting Information) by capital letters.

By comparing BCPs Cl13′···H20, H20···H26′, H18···H30′, and O4···H32′ in 8 Cl-TIBO/Y188 (W) with the equivalent BCPs Cl13′···H20, H20···H26′, H17···H30′, and O4···H30′ in 8 Cl-TIBO/Y188 (M), it can be noted that $\rho_b(r)$ is higher for all the BCPs in the latter dimer. This fact shows that the interaction between the inhibitor and the amino acid is stronger in 8 Cl-TIBO/Y188 (M) than in 8 Cl-TIBO/Y188 (W) dimer.

There are five intermolecular BCPs in 9 Cl-TIBO/Y188 dimer (Table 14 and Figure S7, Supporting Information). All the BCPs have $\rho_b(r)$ and $L(r)$ values in the range proposed by Popelier for the establishment of a hydrogen bond.[79] However, BCP **5** has very high ellipticity, BCPs **1** and **2** have a medium ellipticity, and these three BPs are curved, which indicates that these interactions are unstable.[35,83,84] All the interactions have BCP−RCP distances that are not so short. Despite that, the only interaction that can be considered a hydrogen bond is O4···H30′ because it exhibits low ellipticity, a linear bond path, a reasonable BCP−RCP distance and, most importantly, it is the only one that takes place between a strong proton acceptor (O) and a weak proton donor (C−H). All other interactions are stabilizing C···H and H···H bonds despite their instability.

Results from the AIM analysis show that: (i) the dimers are stabilized mainly by weak C···H and H···H interactions of van der Waals type and also by weak hydrogen bonds of the C−H···O type, (ii) amino acid−inhibitor interactions are stronger in 8 Cl-TIBO/Y188 (W) when compared with 8 Cl-TIBO/Y188 (M). Item (ii) agrees with the NBO analysis, which gives evidence that the mutation Y181C leads to a stronger interaction between the TIBO and Y188, partially compensating for the interactions lost upon substitution of a tyrosine for a cysteine in position 181.

Energetic Analysis. Various researchers have proposed the use of an additional parameter to the Laplacian, to distinguish between the open-shell (covalent bonds) and closed-shell interactions (van der Waals interactions, hydrogen bonds, etc).[93,94] Such a parameter is the total energy density, $H(r)$, given by the following equation:

$$H(r) = G(r) + V(r)$$

where $G(r)$ and $V(r)$ correspond to the kinetic and potential energies densities, respectively. For a covalent bond, the $V(r)$ value, which is negative for any interaction, at the BCP is higher than $G(r)$, which is positive for any interaction, so $H(r)$ is negative. As for the closed-shell interactions, $G(r)$ is higher than $V(r)$, thus $H(r)$ is positive.[91−93] The magnitude of $H(r)$ reflects the covalent character of the interaction.[94,95] Recently, it was proposed to use $-G(r)/V(r)$ as an indicator of shared or closed-shell interactions.[96] If this ratio is greater than 1, the interaction is noncovalent. Between 0.5 and 1, the interaction is partially covalent, and when this ratio is less than 0.5, the interaction is covalent.

For all the dimers studied here, the total energy density is positive (Table S8, Supporting Information), which indicates that all the intermolecular interactions in the dimers exhibit the typical features of a closed-shell interaction because $L(r) < 0$ and $H(r) > 0$.[93,94] It is also noteworthy that the hydrogen bonds in 8 Cl-TIBO/Y181 (W) and 8 Cl-TIBO/C181 (M) (C16−H30′···N1), in 8 Cl-TIBO/K101 (W), 8 Cl-TIBO/K101 (M), and 9 Cl-TIBO/K101 (N1′-H22′···O4 and N1−H11···S4′), in 8 Cl-TIBO/Y188 (W), 8 Cl-TIBO/Y188 (M), and 9 Cl-TIBO/Y188 [C16′−H30′(32′)···O4] exhibit a predominant electrostatic character and no covalent character at all because the total energy density is positive.[97] Only one interaction (C5···H34′) present in 8 Cl-TIBO/Y188 (M) dimer has a very small negative $H(r)$ value [$H(r) = -1.113 \times 10^{-3}$ a.u.], and $-G(r)/V(r)$ slightly less than 1, which gives evidence of a partial covalent character for this interaction.

Conclusions

NBO and AIM analysis of the TIBO/Y181 (C181) interactions showed that the interaction between the inhibitors and the amino acids are stabilized by hydrophobic van der Waals interactions and weak C−H···N hydrogen bonds. Mutation Y181C leads to loss of favorable interactions between the inhibitor and the amino acid in position 181, as seen from the weaker charge transfer and the density values at the BCPs in 8 Cl-TIBO/C181 (M).

As for the TIBO/K101 interaction in the three dimers studied here, both NBO and AIM analysis gave evidence that the dimers are stabilized by an N1···H22′ hydrogen bond, which has been well described in the literature.[3,4,55] The presence of an additional hydrogen bond between atoms S4′ and H11 (S4′···H11), a so-called resonance-induced hydrogen bond, was also observed. Although the S4′···H11 hydrogen bond is weaker than N1···H22′, the former plays an important role in the stabilization of the TIBO−K101 interaction. This is the first time that this hydrogen bond has been reported to take place between a TIBO and K101.

According to the NBO and AIM analyses, the TIBO/Y188 dimers are stabilized mainly by weak van der Waals interactions and weak C−H···O hydrogen bonds. Moreover, the TIBO/Y188 interaction is strongest in 8 Cl-TIBO/Y188 (M) (where mutation Y181C occurs) because the inhibitor is closer to Y188. This must happen as an attempt to partially compensate for the loss of interactions between the inhibitor and the Y181, replaced with a cysteine in the mutant protein.

The NPA analysis and the sum of electronic stabilization energy, $\sum \Delta E^{(2)}$, both obtained by NBO method, together the value of density at BCP obtained from the AIM method, indicate that the Y181C mutation affects the interaction of the inhibitor not only in the position where it occurs but also with the K101

and Y188. In the case of the TIBO/K101 dimers, the interaction of the inhibitor is less effective in the mutant protein. In this same protein, the TIBO/Y188 interaction is stronger. These results show that the loss of favorable interactions between the inhibitor and Y181 cannot be the only cause for the resistance of the reverse transcriptase enzyme to the TIBO inhibitor. It is also necessary to analyze the interaction between the inhibitor and other amino acids in the active site.

The values of $\sum\Delta E^{(2)}$ for the interaction between the TIBO and the Y181 (C181), K101, and Y188 indicate that the 8 Cl-TIBO presents a more effective interaction with these amino acids than 9 Cl-TIBO. Because the 8 Cl-TIBO has a higher biological activity when compared with the 9 Cl-TIBO (IC_{50} = 6 nM and 33 nM, respectively), the later result is quite interesting and it suggests that $\sum\Delta E^{(2)}$ may be used as a qualitative parameter to analyze the differences observed in the biological activity of molecules that bind at same active site.

The presence of the critical points N1···H30′ in 8 Cl-TIBO/Y181 (W) and 8 Cl-TIBO/C181 (M), and O4···H30′ (H32′) in 8 Cl-TIBO/Y188 (W), 8 Cl-TIBO/Y188 (M) and 9 Cl-TIBO/Y188 indicates that these interactions are weak hydrogen bonds. This result could be explored in the development of the new substances that are resistant to Y181C mutation by substitution of hydrogen in the metal group (C16′) for good acceptors and/or donors of hydrogen bonds, like −OH and −NH2 groups. Maybe these substitutions could be used to promote the formation of strong hydrogen bonds between TIBO and the backbone of Y181 and Y188 amino acids, to which the inhibitor will become less susceptible to mutations in these positions because the alterations are made only in the side chains of the amino acids, as long as a great conformational change in the protein with the mutation does not occur.

Acknowledgment. The authors thank the financial support of Brazilian foundations FAPESP, CNPq, and CAPES. R.F.F. acknowledges FAPESP for a master fellowship and S.E.G. thanks CNPq for a research fellowship.

Supporting Information Available: Second-order perturbation energy ($\Delta E^{(2)}$) of the intramolecular interactions taking place in inhibitors from the TIBO family (Table S1). Tables S2−S4 contain all intermolecular interactions taking place in TIBO/amino acid dimers. Tables S5−S7 contain the intramolecular BCP properties for TIBO/amino acid dimers. Table S8 presents the values of $G(r)$, $V(r)$, and $H(r)$ for TIBO/amino acid dimers. Figure S1 contain the atom numbering of 8 Cl-TIBO/C181 (M) dimer. Figures S2−S7 contain the molecular graph for all TIBO/amino acids dimers that are absent in the main text. This material is available free of charge via the Internet at http://pubs.acs.org.

References and Notes

(1) Fauci, A. *Nat. Med.* **2003**, *9*, 839.
(2) *AIDS Epidemic Update: 2004*. Available from: http:/www.unaids.gov/wa2004/report_pdf.html.
(3) Ren, J.; Esnouf, R.; Hopkins, A.; Ross, C.; Jones, Y.; Stammers, D.; Stuart, D. *Structure* **1995**, *3*, 915.
(4) Das, K.; Ding, J.; Hsiou, Y.; Clark, A. D., Jr.; Moereels, H.; Koymans, L.; Andries, K.; Pauwels, R.; Janssen, P. A.; Boyer, P. L.; Clark, P.; Smith, R. H., Jr.; Kroeger, S. M. B.; Michejda, C. J.; Hughes, S. H.; Arnold, E. *J. Mol. Biol.* **1996**, *264*, 1085.
(5) Kohlstaedt, L. A.; Wang, J.; Friedman, J. M.; Rice, P. A.; Steitz, T. A. *Science* **1992**, *256*, 1783.
(6) Smerdon, S. J.; Jager, J.; Wang, J.; Kohlstaedt, L. A.; Chirino, A. J.; Friedman, J. M.; Rice, P. A.; Steitz, T. A. *Proc. Natl. Acad. Sci. U.S.A.* **1994**, *91*, 3911.
(7) Jacobo-Molina, A. J.; Ding, J.; Nanni, R. G.; Clark, A. D., Jr.; Lu, X.; Tantillo, C.; Williams, R. L.; Kamer, G.; Ferris, A. L.; Clark, P. *Proc. Natl. Acad. Sci. U.S.A.* **1993**, *90*, 6320.
(8) Ren, J.; Esnouf, R.; Garman, E.; Somers, D.; Ross, C.; Kirby, L.; Keeling, J.; Darby, G.; Jones, Y.; Stuart, D.; Stammers, D. *Nat. Struct. Biol.* **1995**, *2*, 293.
(9) Esnouf, R.; Ren, J.; Ross, R.; Jones, Y.; Stammers, D.; Stuart, D. *Nat. Struct. Biol.* **1995**, *2*, 303.
(10) Ding, J.; Das, K.; Tantillo, C.; Zhang, W.; Clark, A. D., Jr.; Jessen, S.; Lu, X.; Hsiou, Y.; Jacobo Molina, A.; Andries, K.; Pauwels, R.; Moereels, H.; Koymans, L.; Janssen, P. A. J.; Smith, R. H. J.; Kroeger, K. R.; Michejda, C. J.; Hughes, S. H.; Arnold, E. *Structure* **1995**, *3*, 365.
(11) Unge, T.; Knight, S.; Bhikhabhai, R.; Lovgren, S.; Dauter, Z.; Wilson, K.; Strandber, B. *Structure* **1994**, *2*, 953.
(12) Jorgensen, W. L.; Wang, D. P.; Rizzo, R. C.; Rives, J. T. *Bioorg. Med. Chem. Lett.* **2001**, *11*, 2799.
(13) De Clercq, E. *J. Med. Chem.* **2005**, *48*, 1297.
(14) De Clercq, E. *Biochim. Biophys. Acta* **2002**, *1587*, 258.
(15) Tantillo, C.; Ding, J.; Jacobo-Molina, A.; Nanni, R. G.; Boyer, P. L.; Hughes, S. H.; Pauwels, R.; Andries, K.; Janssen, P. A. J.; Arnold, E. *J. Mol. Biol.* **1994**, *243*, 369.
(16) De Clercq, E. *Farmaco* **1999**, *54*, 26.
(17) Stammers, D. K.; Ren, J.; Nichols, C. E.; Chamberlain, P. P.; Weaver, K. L.; Short, S. A. *J. Mol. Biol.* **2004**, *336*, 569.
(18) Hopkins, A. L.; Ren, J.; Milton, J.; Hassen, R. J.; Chan, J. H.; Stuart, D. I.; Stammers, D. K. *J. Med. Chem.* **2004**, *47*, 5912.
(19) Freeman, G. A.; Andrews, C. W.; Hopkins, A. L.; Lowell, G. S.; Schaller, L. T.; Cowan J. R.; Gonzales, S. S.; Koszalka, G. W.; Hazen, R. J.; Boone, L. R.; Ferris, R. G.; Creech, K. L.; Roberts, G. B.; Short, S. A.; Weaver, K.; Reynolds, D. J.; Milton, Ren, J.; Stuart, D. I.; Stammers, D. K.; Chan, J. H. *J. Med. Chem.* **2004**, *47*, 5923.
(20) Chamorro, C.; Lobaton, E.; Bonache, M. C.; De Clercq, E.; Balzarini, J.; Velásquez, S.; Felix, A. S. *Bioorg. Med. Chem. Lett.* **2001**, *11*, 3085.
(21) Castro, S.; Lobaton, E.; Perez, M. J. P.; Felix, A. S.; Cordeiro; A., Andrei; G., Snoeck, R.; De Clercq, E.;, Balzarini, J.; Camarasa, M. J.; Velázquez, S. *J. Med. Chem.* **2005**, *48*, 1158.
(22) Lindberg, J.; Sigurosson, S.; Lowgren, S.; Andersoon, H. O.; Sahlber, C.; Noreen, R.; Fridborg, K. *Eur. J. Biochem.* **2002**, *269*, 1670.
(23) Ren, J.; Nichols, C.; Bird, L.; Chamberlain, P.; Weaver, K.; Short, S.; Stuart, D. I.; Stammers, D. K. *J. Mol. Biol.* **2001**, *312*, 795.
(24) Pata, J. D.; Stirtan, W. G.; Goldstein, S. W.; Steitz, T. A. *Proc. Natl. Acad. Sci. U.S.A.* **2004**, *101*, 10548.
(25) Ren, J.; Milton, J.; Weaver, K. L.; Short, S. A.; Stuart, D. I.; Stammers, D. K. *Structure* **2000**, *8*, 1089.
(26) Rizzo, R. C.; Wang, D. P.; Tirado-Rives, J.; Jorgensen, W. L. *J. Am. Chem. Soc.* **2000**, *122*, 12898.
(27) Hsiou, Y.; Das, K.; Ding, J.; Clark, A. D.; Moereels, H. *Structure* **2001**, *4*, 853.
(28) Blagovic, M. U.; Tirado-Rives, J.; Jorgenssen, W. L. *J. Am. Chem. Soc.* **2003**, *125*, 6016.
(29) Das, K.; Clark, A. D., Jr.; Lewi, P. J.; Heeres, J.; de Jonge, M. R.; Koymans, L. M. H.; Vinkers, H. M.; Daeyaert, F.; Ludovici, D. W.; Kukla, M. J.; De Corte, B.; Kavash, R. W.; Ho, C. Y.; Ye, H.; Lichtenstein, M. A.; Andries, K.; Pauwels, R.; de Bethune, M.-P.; Boyer, P. L.; Clark, P.; Hughes, S. H.; Janssen, P. A. J.; Arnold, E. *J. Med. Chem.* **2004**, *47*, 2550.
(30) Meyer, E. A.; Castellano, R. K.; Diederich, F. *Angew. Chem., Int. Ed.* **2003**, *42*, 1210.
(31) Hunter, C. A.; Lawson, K. R.; Perkins, J.; Urch, C. J. *J. Chem. Soc., Perkin Trans. 2* **2001**, 651.
(32) Brandl, M.; Weiss, M. S.; Jabs, A.; Suhnel, J.; Hilgenfeld, R. *J. Mol. Biol.* **2001**, *307*, 357.
(33) Reed, A. E.; Curtis, L. A.; Weinhold, F. *Chem. Rev.* **1988**, *88*, 899.
(34) Reed, A. E.; Weinstock, R. B.; Weinhold, F. *J. Chem. Phys.* **1985**, *83*, 735.
(35) Bader, R. F. W. *Atoms in Molecules—A Quantum Theory*; International Series of Monographs on Chemistry, No. 22; Oxford University Press: Oxford, 1990.
(36) Berman, H. M.; Westbrook, J.; Feng, Z.; Gilliland, G.; Bhat, T. N.; Weissig, H.; Shindyalov, I. N.; Bourne, P. E. *Nucl. Acid Res.* **2000**, *28*, 235.
(37) Sayle, R. *Molecular Graphics Visualization Tool*; Glaxo Research and Development: Greeford, Middlesex, U.K., 1994.
(38) Gosper, J. J. *BabelWin, A Molecular Structure Information Interchange Hub*; Brunel University: London, 1998.
(39) Schaftenaar, G.; Noordik, J. H. *J. Comput.-Aided Mol. Des.* **2000**, *14*, 123.
(40) Lee, C.; Yang, W.; Parr, R. G. *Phys. Rev. B* **1988**, *37*, 785.
(41) Frisch, M. J.; Trucks, G. W.; Schlegel, H. B.; Scuseria, G. E.; Robb, M. A.; Cheeseman, J. R.; Zakrzewski, V. G.; Montgomery, J. A., Jr.; Stratmann, R. E.; Burant, J. C.; Dapprich, S.; Millam, J. M.; Daniels, A. D.; Kudin, K. N.; Strain, M. C.; Farkas, O.; Tomasi, J.; Barone, V.; Cossi, M.; Cammi, R.; Mennucci, B.; Pomelli, C.; Adamo, C.; Clifford, S.; Ochterski, J.; Petersson, G. A.; Ayala, P. Y.; Cui, Q.; Morokuma, K.; Malick, D. K.; Rabuck, A. D.; Raghavachari, K.; Foresman, J. B.; Cioslowski, J.;

Ortiz, J. V.; Stefanov, B. B.; Liu, G.; Liashenko, A.; Piskorz, P.; Komaromi, I.; Gomperts, R.; Martin, R. L.; Fox, D. J.; Keith, T.; Al-Laham, M. A.; Peng, C. Y.; Nanayakkara, A.; Gonzalez, C.; Challacombe, M.; Gill, P. M. W.; Johnson, B. G.; Chen, W.; Wong, M. W.; Andres, J. L.; Head-Gordon, M.; Replogle, E. S.; Pople, J. A. *Gaussian 98*, revision A.9; Gaussian, Inc.: Pittsburgh, PA, 1998.

(42) Glendening, E. D.; Badenhoop, J. K.; Reed, A. E.; Carpenter, J. E.; Bohmann, J. A.; Morales, C. M.; Weinhold, F. *NBO 5.0*; Theoretical Chemistry Institute, University of Wisconsin: Madison, WI, 2001.

(43) König, F. B.; Schönbohm, J.; Bayles, D. *J. Comput. Chem.* **2001**, *22*, 545.

(44) Pettersen, E. F.; Goddard, T. D.; Huang, C. C.; Couch, G. S.; Greenblatt, D. M.; Meng, E. C.; Ferrin, T. E. *J. Comput. Chem.* **2004**, *25*, 1605.

(45) Freitas, R. F.; Galembeck, S. E. *Chem. Phys. Lett.* **2006**, *423*, 131.

(46) Abrahão-Junior, O.; Nascimento, P. G. B. D.; Galembeck, S. E. *J. Comput. Chem.* **2001**, *22*, 1817.

(47) Goodman, J. M.; Still, W. C. *J. Comput. Chem.* **1991**, *12*, 1110.

(48) Desiraju, G. R. *Acc. Chem. Res.* **2002**, *35*, 565.

(49) Shishkin, O. V.; Elstner, M.; Frauenheim, T.; Suhai, S. *Int. J. Mol. Sci.* **2003**, *4*, 537.

(50) Brandl, M.; Lidauer, K.; Meyer, M.; Sühnel, J. *Theor. Chem. Acc.* **1999**, *101*, 103.

(51) Marjo, C. E.; Bishop, R.; Craig, D. C.; Scudder, M. L. *Eur. J. Org. Chem.* **2001**, *5*, 863.

(52) Saen-oon, S.; Kuno, M.; Hannongbua, S. *Proteins* **2005**, *61*, 859.

(53) Domagała, M.; Grabowski, S. J.; Urbaniak, K.; Mlostoń, G. *J. Phys. Chem. A* **2003**, *107*, 2730.

(54) Taylor, R.; Kennard, O. *J. Am. Chem. Soc.* **1982**, *104*, 5063.

(55) De Corte, B. L. *J. Med. Chem.* **2005**, *48*, 1689.

(56) Domagała, M.; Grabowski, S. J.; Urbaniak, K.; Mlostoń, G. *J. Mol. Struct.* **2004**, *690*, 69.

(57) Jansen, P. A. J.; Lewi, P. J.; Arnold, E.; Daeyaert, F.; Jonge, M.; Heeres, J.; Koymans, L.; Vinkers, M.; Guillemont, J.; Pasquier, E.; Kukla, M.; Ludovici, D.; Andries, K.; Béthune, M. P.; Pauwels, R.; Das, K.; Clark, A. D., Jr.; Frenkel, Y. V.; Hughes, S. H.; Medaer, B.; De Knaep, F.; Bohets, H.; De Clerck, F.; Lampo, A.; Williams, P.; Stoffels, P. *J. Med. Chem.* **2005**, *48*, 1901.

(58) Wang, D. P.; Rizzo, R. C.; Rives, J. T.; Jorgensen, W. L. *Bio. Med. Chem. Lett.* **2001**, *11*, 2799.

(59) Smith, R. H. J.; Jorgensen, W. L.; Rives, J. T.; Lamb, M. L.; Janssen, P. A.; Michejda, C. J.; Smith, M. B. K. *J. Med. Chem.* **1998**, *41*, 5272.

(60) Allen, F.; Bird, C. M.; Rowland, R. S.; Raithby, P. R. *Acta Crystallogr., Sect. B* **1997**, *53*, 680.

(61) Martinez, J. V.; Ortega, S. H.; Rubio, M.; Li, D. T.; Swearingen, J. K.; Kaminsky, W.; Kelman, D. R.; West, D. X. *J. Chem. Crystallogr.* **2004**, *34*, 8, 533.

(62) Venkatachalam, T. K.; Sudbeck, E.; Uckun, F. M. *J. Mol. Struct.* **2004**, *687*, 45.

(63) Li, Q.; Mak, T. C. W. *Acta Crystallogr., Sect. B* **1997**, *53*, 252.

(64) Li, Q.; Mak, T. C. W. *Acta Crystallogr., Sect. B* **1996**, *52*, 989.

(65) Seth, S.; Biswas, A.; Banerjee, A.; Chattopadhay, S. K.; Ghosh, S. *Acta Crystallogr., Sect. C* **1996**, *52*, 2377.

(66) Ramnathan, A.; Sivakumar, K.; Subramanian, K.; Meerarani, D.; Ramadas, K.; Fun, H. K. *Acta Crystallogr., Sect. C* **1996**, *52*, 139.

(67) Ramnathan, A.; Sivakumar, K.; Subramanian, K.; Meerarani, D.; Ramadas, K.; Fun, H. K. *Acta Crystallogr., Sect. C* **1996**, *52*, 656.

(68) Ramnathan, A.; Sivakumar, K.; Subramanian, K. *Acta Crystallogr., Sect. C* **1995**, *51*, 2446.

(69) Lee, C. R.; Tang, T. H.; Chen, L.; Wang, C. C.; Wang, Y. *J. Phys. Chem. Solids* **2004**, *65*, 1957.

(70) Bharatam, P. V.; Amita, A. G.; Kaur, D. *Tetrahedron* **2002**, *58*, 1759.

(71) Wennmohs, F.; Staemmler, V.; Schindler, M. *J. Chem. Phys.* **2003**, *119*, 3208.

(72) François, S.; Rohmer, M. M.; Benard, M.; Moreland, A. C.; Rauchfuss, T. B. *J. Am. Chem. Soc.* **2000**, *122*, 12743.

(73) Desiraju, G. R. *Acc. Chem. Res.* **1991**, *24*, 290.

(74) Derewenda, Z. S.; Derewenda, U.; Kobos, P. *J. Mol. Biol.* **1994**, *241*, 83.

(75) Derewenda, Z. S.; Lee, L.; Derewenda, U. *J. Mol. Biol.* **1995**, *252*, 248.

(76) Jiang, L.; Lai, L. *J. Biol. Chem.* **2002**, *277*, 37732

(77) Pierce, A. C.; Sandretto, K. L.; Bemis, G. W. *Proteins* **2002**, *49*, 567.

(78) Sarkhel, S.; Desiraju, G. R. *Proteins* **2004**, *54*, 247.

(79) Popelier, P. *Atoms in Molecules: An Introduction*; Prentice Hall: New York, 2000.

(80) Matta, C. F.; Bader, R. F. W. *Proteins* **2000**, *40*, 310.

(81) Cioslowski, J.; Mixon, S. T. *J. Am. Chem. Soc.* **1992**, *114*, 4382.

(82) (a) Matta, C. F.; Trujillo, J. H.; Tang, T. H.; Bader, R. F. W. *Chem.—Eur. J.* **2003**, *9*, 1940. (b) Matta, C. F.; Castillo, N.; Boyd, R. J. *J. Phys. Chem. B* **2006**, *110*, 563−578.

(83) Cremer, D.; Kraka, E.; Slee, T. S.; Bader, R. F. W.; Lau, C. D. H.; Nguyen-Ding, T. T.; MacDougall, P. J. *J. Am. Chem. Soc.* **1983**, *105*, 5069.

(84) Bader, R. F. W.; Slee, T. S.; Cremer, D.; Kraka, E. *J. Am. Chem. Soc.* **1983**, *105*, 5061.

(85) Vila, A.; Mosquera, R. A. *Chem. Phys.* **2003**, *291*, 73.

(86) Aakeröy, C. B.; Evans, T. A.; Seddon, K. R.; Pálinko, I. *New J. Chem.* **1999**, 23, 145.

(87) Keegstra, E. M. D.; Spek, A. L.; Zwikker, J. W.; Jenneskens, L. W. *J. Chem. Soc., Chem. Commun.* **1994**, *14*, 1633.

(88) Steiner, T.; Saenger, W. *J. Chem. Soc., Chem. Commun.* **1995**, *20*, 2087.

(89) Balamurugan, V.; Jacob, W.; Mukherjee, J.; Mukherjee, R. *Cryst. Eng. Commun.* **2004**, *6*, 396.

(90) Müller, G.; Lutz, M.; Harder, S. *Acta Crystallogr.* **1996**, *52*, 1014.

(91) Grabowski, S. J. *J. Phys. Org. Chem.* **2004**, *17*, 18.

(92) Bone, R. G. A.; Bader, R. F. W. *J. Phys. Chem.* **1996**, *100*, 10892.

(93) Macchi, P.; Proserpio, D. M.; Sironi, A. *J. Am. Chem. Soc.* **1998**, *120*, 13429.

(94) Koch, W.; Frenking, G.; Gauss, J.; Cremer, D.; Collins, J. R. *J. Am. Chem. Soc.* **1987**, *109*, 5917.

(95) Cramer, D.; Kraka, E. *Angew. Chem., Int. Ed. Engl.* **1984**, *23*, 627.

(96) Ziółkowski, M.; Grabowski, S. J.; Leszczynski, J. *J. Phys Chem. A* **2006**, *110*, 6514.

(97) Rozas, I.; Alkorta, I.; Elguero, J. *J. Am. Chem. Soc.* **2000**, *122*, 11154.